

FDMA in Point-to-Multipoint Fibre Access Systems for Non-Residential Applications

Original

FDMA in Point-to-Multipoint Fibre Access Systems for Non-Residential Applications / Cano, Ivan N.; Caruso, Giuseppe; Wei, Jinlong; Talli, Giuseppe; Bluemm, Christian; Calabro, Stefano; von Kirchbauer, Heinrich; Wuensche, Ullrich; Leyva, Pablo; Rongfang, Huang; Zhang, Kuo; Ye, Zhicheng. - ELETTRONICO. - (2023), pp. 1-4. (2023 23rd International Conference on Transparent Optical Networks (ICTON) Bucharest, Romania 02-06 July 2023) [10.1109/icton59386.2023.10207353].

Availability:

This version is available at: 11583/2981104 since: 2023-09-05T09:17:08Z

Publisher:

IEEE

Published

DOI:10.1109/icton59386.2023.10207353

Terms of use:

This article is made available under terms and conditions as specified in the corresponding bibliographic description in the repository

Publisher copyright

IEEE postprint/Author's Accepted Manuscript

©2023 IEEE. Personal use of this material is permitted. Permission from IEEE must be obtained for all other uses, in any current or future media, including reprinting/republishing this material for advertising or promotional purposes, creating new collecting works, for resale or lists, or reuse of any copyrighted component of this work in other works.

(Article begins on next page)

on the uplink in this paper since we envision that the traffic will flow mainly in this direction. However, a full downlink and uplink FDMA system has been reported in [7] for a future residential PON. The Rx in the OAP is based on a commercial ICR which allows to have high Rx sensitivity and separate the OTE spectra electrically by means of digital signal processing (DSP) [3]-[5]. In the OTE, we employ directly modulated laser (DML) as a low-cost solution Tx, potentially for sensors or cameras. We show the detection of 3 OTEs simultaneously at bitrates of 2.5 Gb/s, 5 Gb/s and 8 Gb/s with Rx sensitivities of -43.5 dBm, -40 dBm, and -34 dBm, respectively, at a pre-FEC BER threshold of 10^{-3} corresponding to RS(255,223) coding with 14.35% overhead and 6.56 dB net coding gain, which is adopted in 10G-EPON. The effect of additional channels, power imbalance and wavelength stability are also presented.

2. EXPERIMENTAL SETUP

Fig. 2 depicts the experimental setup. We firstly generate offline three set of random bit sequences at 2.5 Gb/s, 5 Gb/s, and 8 Gb/s, encode them differentially, and shape them by a root-square raised cosine (RRC) filter with roll-off factor of 0.05. We then upsample the signal and apply a differentiator with a half-bit delay function. The latter is used to obtain a phase-modulated signal from the DML [9], [10]. The real-valued waveforms are loaded into a digital to analogue converter (DAC) with sampling rate of 80 GSa/s. The three electrical signals are amplified and directly modulate three distributed feedback laser (DFB) whose emission wavelengths are tuned and controlled in temperature. By means of a centralized control system, we set the wavelength of each DFB to a different value in order to avoid interference. We then combine the three optical signals through optical couplers and control their power independently through variable optical attenuators (VOA). The whole signal propagates through 20km of single mode fibre (SMF) and another VOA controls the total input power into the ICR. As local oscillator (LO) we use an external cavity laser (ECL), which is effectively the reference for the wavelength control system of the OTE Tx. The four outputs of the ICR with the in-phase and quadrature information in both polarizations are then quantized by the analogue to digital converters (ADC) embedded in a real-time oscilloscope and further processed offline. The Rx DSP comprises a tributary de-skewing followed by an electrical frequency down-conversion of the three detected signals. Once the three signals are in baseband they are low-pass filtered and down-sampled. The resulting real data stream goes through an automatic gain control (AGC), a 4×2 multiple input and multiple output (MIMO) equalizer [11] and carrier phase recovery (CPR) stage. Finally, the BER is calculated by direct error counting.

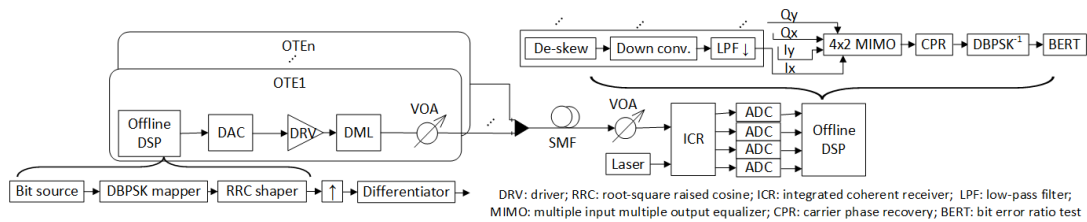


Fig. 2: Experimental setup of upstream coherent FDM P2MP network using DML and transceiver offline DSP.

The ICR is also used to determine the wavelength of each OTE with reference to the LO wavelength. Each DML has a TEC controlled by a consumer micro-controller, which is used to control and tune its wavelength according to the information on the relative wavelength error provided by the OAP Rx. During registration, the OAP first indicates the OTEs to move to the highest possible wavelength by heating. Then, the OTEs slowly cool down and are detected in a registration channel. The OAP then indicates each OTE their current wavelength and where to move following the $0.1\text{nm}/^\circ\text{C}$ rule of thumb for DFBs. Once the DMLs are at the correct separation, they transmit information and the OAP continuously monitors and controls their wavelength in a closed loop.

3. RESULTS

The spectrum of the three detected OTE signals after the ADC is shown in Fig. 3. The three signals have the same optical power and Fig. 3(a) and 3(b) display the signals with either a spectral gap or no gap between OTEs, respectively. The OTE data rates are 8 Gb/s, 2.5 Gb/s, and 5 Gb/s (as indicated in Fig. 3 from left to right on the detected signal spectrum). We test different data rates for each OTE to emulate the varying BW demand of OTEs in a real network. We add an extra dummy channel with 12.5 dB higher power than the others, as shown in Fig. 3(c) to emulate a full capacity network as well as possible power difference in P2MP networks due to different optical splitting or launch powers.

The BER vs. received optical power (ROP) performance of DBPSK signals at several experimental configurations is shown in Fig. 4. We firstly measure each channel independently in optical back-to-back (oBtB). At a BER of 10^{-3} , we measure an Rx sensitivity of -45.5 dBm for the 2.5 Gb/s OTE and the 5 Gb/s and 8 Gb/s have penalties of 4.7 dB and 9 dB respectively. While these penalties exceed the theoretical 3 dB and 5 dB for increasing the bitrate, these are explained by the limited BW of the electrical components and the DMLs.

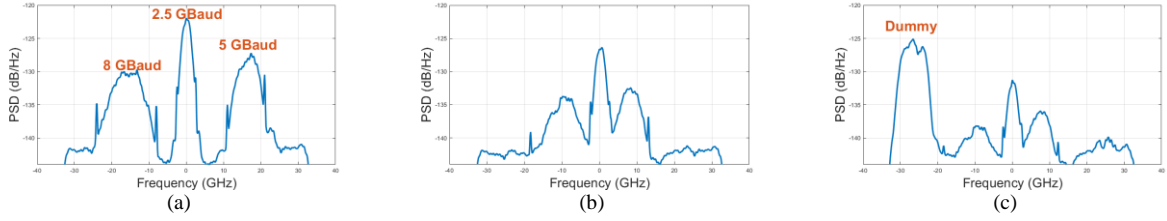


Fig. 3: Spectra of the detected signal with equalized power with (a) and without (b) spectral gap; (c) an additional channel emulating full capacity is added.

We then join the three signals at same optical power and with the centre frequencies separated by 16 GHz, which leaves a spectral gap between adjacent channels as can be seen in Fig. 3(a). After detecting the three signals simultaneously in the ICR, we observe no penalty for the 2.5 Gb/s and 5 Gb/s relative to the independent channel measurement. On the other hand, the 8 Gb/s has 1 dB penalty mainly caused by slight interference from the neighbour channel. Since we apply a strong spectral shaping, we can suppress the spectral gap between the channels (Fig. 3(b)). In this case, there is a penalty of 1 dB for both the 2.5 Gb/s and 5 Gb/s OTEs, and of 1.8 dB for the 8 Gb/s OTE. This penalty is because even with strong shaping in Tx, there is some residual interference between the channels which further indicates the importance of the wavelength control to stabilize the OTE frequency to avoid strong drifts. In our demonstration employing the accurate closed loop thermal tuning and stabilization wavelength drift of less than ± 50 MHz has been measured over an extended time [12].

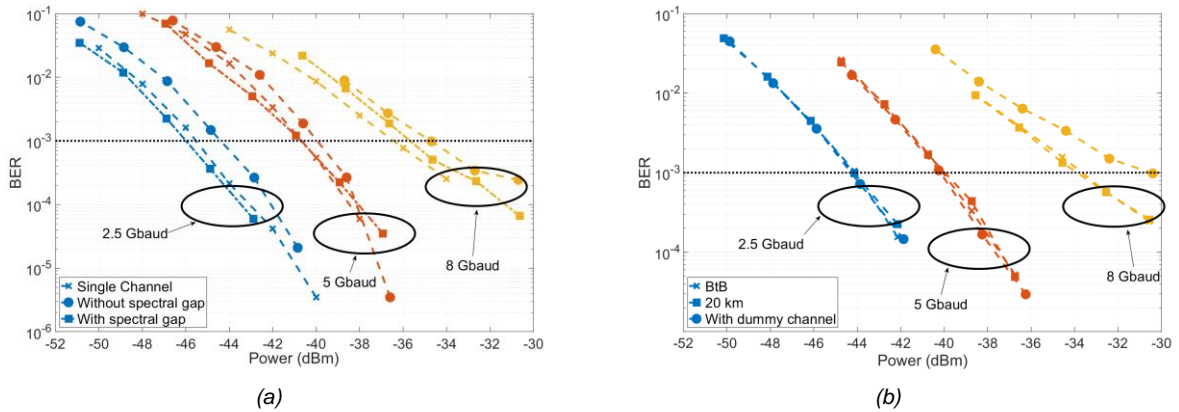


Fig. 4: BER vs. ROP performance for each OTE: (a) impact from channel spectral gap in oBtB; and (b) transmission over 20 km SMF.

In Fig. 4(b) we plot the performance after 20 km SMF transmission. There is no penalty with respect to oBtB, since the symbol rates of the DBPSK signals are relatively low. We obtain power sensitivities of -43.5 dBm, -40 dBm, and -34 dBm for 2.5 Gb/s, 5 Gb/s and 8 Gb/s DBPSK signals, respectively. Fig. 4(b) also shows the impact of having the network at full capacity emulated by adding a dummy channel (Fig. 3(c)) without spectral gap. We observe no penalty for both 2.5 Gb/s and 5 Gb/s signals compared with the case of having only the three OTE signals since the system is limited by shot noise rather than ADC quantization noise. However, the 8 Gb/s OTE shows about 4 dB penalty as part of the emulated dummy channel interferes in the spectrum as seen in Fig. 3(c).

Despite having demonstrated only 3 DML-based OTEs for an overall data rate of 15.5 Gb/s, 3 additional OTEs could be easily allocated in the 60 GHz optical BW system. Alternatively, if all OTEs operate at 2.5 Gb/s, 12 OTEs could be supported for an overall capacity of 30 Gb/s. Further scaling the system up to 60 or 120 Gb/s could be achieved by employing either wider BW ICR or by using higher modulation formats like differential quadrature PSK (DQPSK) or adding polarization multiplexing.

As mentioned above, the wavelength control is of high importance in the proposed architecture. Fig. 5(a) shows the spectra of two OTEs whose emission frequency is monitored and controlled at the OAP. Each of the OTE signals is measured after applying a fast-Fourier transform (FFT) to the samples obtained through the ICR using the LO as reference. We insert a pilot tone in the transmitted signals for identifying the OTEs and aid the wavelength estimation. The pilot tones are located by searching a peak in the spectrum. Then, they are monitored and controlled within ± 50 MHz by sending commands to a Raspberry Pi in the OTE to control its temperature. The minimum frequency window depends on the number of points of the FFT and the repetition rate that is needed.

We further explore the possibility of sharing a frequency channel by using TDM as illustrated in Fig. 5(b). For this experiment, we use three optical modulators, each with a different DFB as light source. Two OTE Tx share a channel and transmit in burst mode while the third one is on an adjacent channel sending data in continuous mode. The bitrate for each OTE is 8 Gb/s with DBPSK format. For the TDM, we add 20 km of SMF in one of

the OTE to delay the burst, so that it can be detected in its corresponding time slot. By using the SMF, we also emulate the transmission effect and different OTE powers arriving into the ICR. Fig. 5(a) depicts the bursts and Fig. 5(c), the Rx graphical unit interface (GUI) of the ICR showing the proper detection of the three OTEs.

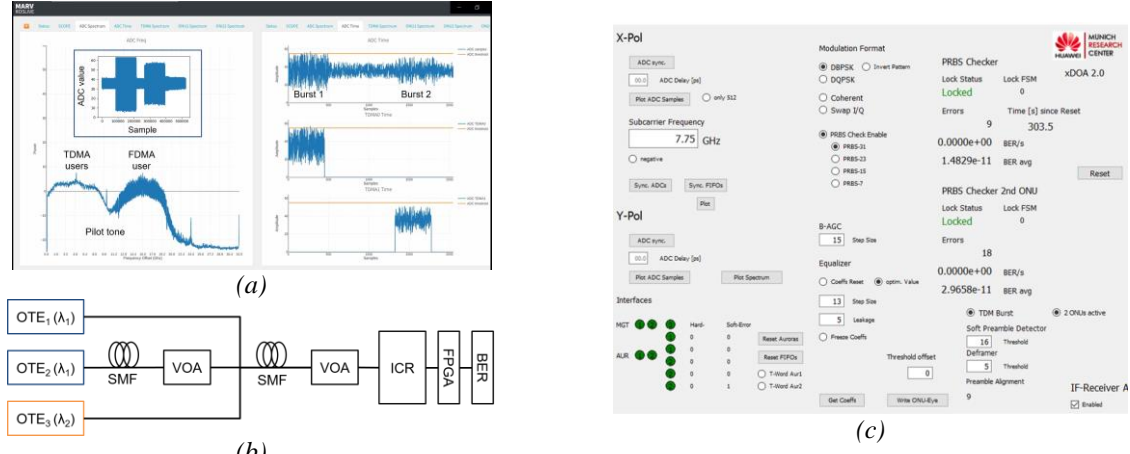


Fig. 5 (a) Wavelength control interface and burst received at the OAP; (b) TDMA and FDMA experimental block diagram; (c) Rx GUI with two TDM users detected

As a final remark, in [12] we demonstrated live Ethernet services in a similar setup as the one studied here but with real-time processing. The total latency of the system measured through clock cycles (~4 ns) of a field-programmable gate array (FPGA) was about 2.5 μs, showing that the proposed system can help on keeping a determinist latency.

4. CONCLUSIONS

We experimentally demonstrated a FDM P2MP upstream transmission system using low-cost 2 GHz DMLs at OTEs with flexible bit rates. The impact of channel gap and power distribution were also examined. By considering a pre-FEC threshold BER of 10^{-3} , we achieved Rx sensitivities of -43.5 dBm, -40 dBm and -34 dBm at 2.5 Gb/s, 5 Gb/s, and 8 Gb/s respectively with DBPSK modulation. No transmission penalty was measured after 20km of fibre. The results show the feasibility of such architecture is allowing several users to transmit simultaneously and a deterministic latency of ~2.5 μs has been measured. Furthermore the capacity of the individual FDM channels can be shared using TDM which allows a more flexible and efficient allocation of the system capacity for the OTEs that do not have strict latency requirements.

REFERENCES

- [1] ETSI, “White paper: The fifth generation fixed network (F5G): bringing fibre to everywhere and everything” (2020)
- [2] Ernst & Young, “White paper: The backbone of digital economies: the revolution of global industries through optical communications” (2021)
- [3] D. Lavery, *et al.*, “Opportunities for optical access network transceivers beyond OOK [invited],” *Journal of Optical Communications and Networking*, vol. 11, pp.A186 - A195, Feb. 2019.
- [4] N. Kaneda, *et al.*, “Coherent PON: System Merit and Technical Challenges,” *Proc. OECC*, Hong Kong, Hong Kong, July 2021, paper W2B.1.
- [5] Z. Zhou, *et al.*, “Multipoint-to-point data aggregation using a single receiver and frequency-multiplexed intensity-modulated ONUs,” *Proc. OFC*, San Diego, CA, Mar. 2022, paper Tu2G.4.
- [6] D. Lavery, *et al.*, “A 32×10 Gb/s OLT using a single ultra-wide bandwidth dual local oscillator coherent receiver,” *Proc. IEEE Photonics Conference Part II*, Orlando FL, Oct. 2017.
- [7] Z. Xing, *et al.*, “First real-time demonstration of 200G TFDMA coherent PON using ultra-simple ONUs,” *Proc. OFC*, San Diego, CA, Mar. 2023, paper Th4C.4.
- [8] N. Shibata, *et al.*, “Time Sensitive Networking for 5G NR Fronthauls and Massive IoT Traffic,” *J. Lightwave Technol.*, vol. 39, pp. 5336-5343, Aug. 2021.
- [9] D. Che, *et al.*, “Enabling Complex Modulation of Directly Modulated Signals Using Laser Frequency Chirp,” *IEEE Photon. Technol. Lett.*, vol. 27, pp. 2407 – 2410, Aug. 2015.
- [10] I. N. Cano, *et al.*, “Direct phase modulation DFBs for cost-effective ONU transmitter in udWDM PONs,” *IEEE Photon. Technol. Letters*, vol. 26, pp. 973–975, Mar. 2014.
- [11] J. Wei, N. Stojanovic, and C. Xie, “Nonlinearity mitigation of intensity modulation and coherent detection systems,” *Optic Letters*, vol. 43, pp. 3148-3151, July 2018.
- [12] C. Bluemm, *et al.*, “FDMA point-to-multi-point fibre access system for latency sensitive applications,” *proc. ECOC*, Basel, Switzerland, Sept. 2022, paper Tu2.2.